ULTRA-HARD DIAMENE FILMS ON SILICON CARBIDE FOR MECHANICAL APPLICATIONS

Filippo Cellini, Francesco Lavini, Elisa Riedo

New York University, Tandon School of Engineering, Brooklyn, NY 11201, USA

ABSTRACT

Similarly to graphite, atomically thin graphene films are known to be extremely flexible, exhibit a large in-plane stiffness (~1TPa), and be quite soft in the direction perpendicular to the graphene layers (~30 GPa). However, contrary to expectations, we found that at room temperature under pressure an epitaxial graphene film composed of buffer layer plus one graphene layer on SiC(0001) behaves at the nanoscale as a diamond-hard coating, which we named diamene. This ultra-thin and ultra-hard film exhibits exceptional mechanical responses to nano-indentation, equal, or even superior, to those of a CVD diamond film. Here, we review recent advancements in the study of diamene films, towards implementation of diamene coatings in current state-of-the-art mechanical technologies.

1. INTRODUCTION

Numerous technological and scientific efforts are underway to leverage the properties of two-dimensional (2D) materials as building blocks in the design of novel integrated nano-electronic and photonic circuits, composites, coatings, and micro- and nano-electro-mechanical systems (MEMS/NEMS). While several experiments and theoretical calculations have revealed exciting novel properties of these nanostructures, many technological questions remain open [1]. A deeper understanding of the mechanical properties of 2D materials is of key importance to enable the development of new nanotechnologies [2].

In recent years, several studies have been dedicated to understand the mechanics of nanomaterials, such as carbon nanotubes [3] and oxide nanobelts [4], while more recently new efforts are underway to study the properties of two-dimensional materials, such as graphene and MoS_2. These ultra-thin films, only few-atomic-layer thick, hold great potential for technological applications [5]. The most studied 2D material is graphene, which exists as a single layer of graphite or a few-layer thick epitaxial graphene film [6]. Graphene possesses a large in-plane elastic modulus, high intrinsic carrier mobility, and high in-plane thermal conductivity. Other than graphene, 2D films of graphene oxide (GO), hexagonal Boron Nitride (h-BN), transition metal dichalcogenides (TMDs), and their heterostructures also hold great promise for nanotechnology applications [7].

SAMPE Conference Proceedings. Charlotte, NC, May 20-23, 2019. Society for the Advancement of Material and Process Engineering – North America.

The development of materials with exceptional mechanical properties has been the focus of a continuous research effort in the history of technology, and synthesizing materials with stiffness and hardness comparable to diamond is a topic of great technological interest. Recently, experimental and theoretical efforts have been directed to study the phase transformation of multi-layer graphene into a diamond-like structure, as induced by chemical functionalization of the graphene layers [8-10]. Novel reports demonstrated that under localized pressure, an atomically-thin graphene film grown on SiC(0001) behaves as a diamond-hard coating, exhibiting mechanical responses to nano-indentation comparable to those of a diamond substrate [11, 12].

These investigations required performing indentations on supported 2D films with indentations smaller than one Ångström. Modulated Å-indentation (ÅI), which is an experimental technique based on the atomic force microscope (AFM), was employed to achieve sub-Å indentation depths during force-indentation measurements on a single layer (1L) of graphene on top of the carbon interfacial layer (buffer layer, BfL), both epitaxially grown on the Si-face of SiC(0001) by Si sublimation. Experiments demonstrate that at room temperature, upon indentation, the single layer graphene film on buffer layer exhibits an indentation stiffness equal or larger than that of bulk diamond, it is resistant to perforation by a diamond indenter and it shows a reversible drop in electrical conductivity upon indentation. In addition to these key results, experiments and calculations showed that the few-layer graphene film transforms into a diamond-like structure only in the region under localized pressure, maintaining the rest of the film in the graphitic-flexible state [11]; furthermore, the surface stiffening effect is reversible and it is observed only for films consisting of one layer plus buffer layer in epitaxial graphene films and is currently not observed on exfoliated graphene flakes on SiO_2 [13].

In this paper, we review recent advancements in the study of the nanomechanics of few-layer epitaxial graphene films, towards implementation of diamene coatings in current state-of-the-art mechanical technologies. In what follows, we initially describe the structure and properties of epitaxial graphene and we introduce the Å-indentation procedure that has been developed to measure the transverse elasticity of 2D films [11, 14] and nanostructures [15], as well as a machine learning method (spectral clustering) to rapidly identify the morphology of graphene layers from friction force microscopy and phase imaging data. In the Results section, we present experimental measurements of the nanomechanical properties of few-layer graphene and diamene films on SiC. We also report relevant results on the identification of graphene domains using the spectral clustering algorithm. In the Conclusion, we discuss current objectives of this research and new directions for implementation of this ultra-stiff ultra-hard films in mechanical technology.

2. EXPERIMENTATION

2.1 Epitaxial graphene films and their structure

Epitaxial graphene films employed in our experiments have been prepared by collaborators (see Acknowledgments) following the confinement controlled sublimation (CCS) method, which is described in the seminal work in Reference [16]. The structure of the epitaxial graphene layers grown on the Si-face of SiC is displayed in Figure 1(a), where we report a TEM micrograph measured at the interface between the SiC substrate and the first few graphene layers. In the

lower part of the micrograph, we observe the crystalline structure of SiC, with the Si atoms clearly visible in the lattice [17]. The few-layer graphene film is also observable on the upmost surface of the sample. A complete graphitic layer partially bonded to the underlying SiC structure lays at the interface between the first graphene layer and the SiC, which is commonly referred as the buffer layer (BfL). This layer has been the object of several fundamental studies over the years and its structure and function in determining the properties of epitaxial graphene films are still under investigation [18].

In Figure 1(b), we display a schematic of the crystalline structure of the 1L graphene film on BfL, where the structures of SiC, BfL and 1L graphene are indicated. Notably, while the BfL shares a very similar crystalline structure with the adjacent graphene layer, the covalent bonds and strong interaction with the underlying SiC crystal confer to this layer properties and morphology that are completely different from those of graphene. The Raman spectra of Silicon Carbide (SiC(0001) crystal) and few-layer graphene films - films composed of large areas of 1L graphene on BfL together with smaller regions of bare BfL and 2L graphene on BfL - are displayed in Figure 1(c). The spectrum of the epitaxial graphene film shares several similarities with the spectrum of the underlying SiC film, due to the partial overlap of the spectrum of pure graphene and the spectrum of SiC [19]. The characteristic peaks of graphene are identified in the spectrum of epitaxial graphene. In particular, we identify the G peak of graphene around 1600 cm^{-1}, which arises from the stretching of the C-C bond in graphitic materials (this peak is present in multilayer graphene and bulk graphite as well as in single layer graphene), and the 2D peak around 2720 cm^{-1}, which is associated to an overtone of the in plane breathing mode - also known as D peak - which is instead activated in graphene structures only in the presence of

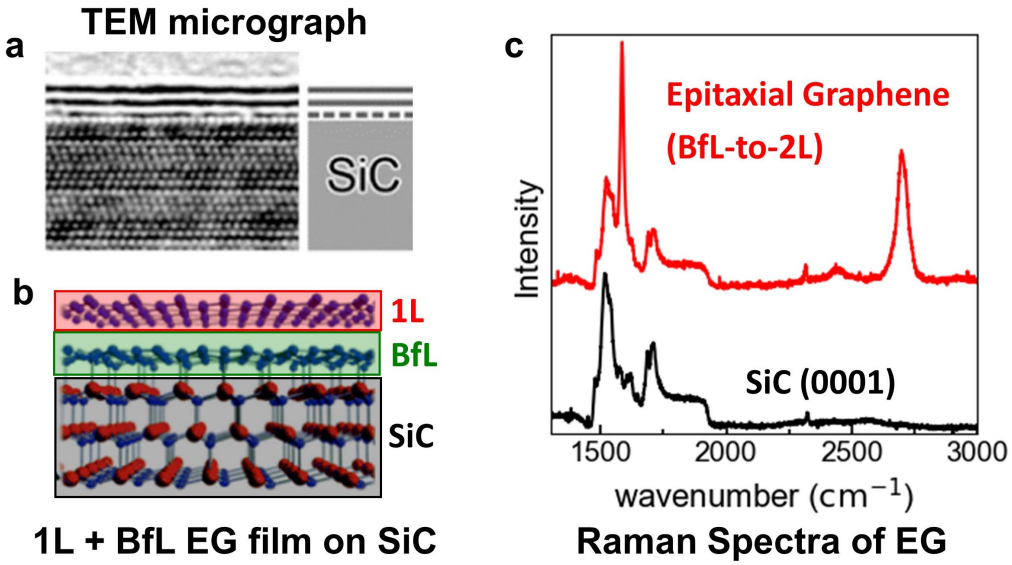

Figure 1. Structure and Raman spectra of Silicon Carbide (SiC), Buffer Layer (BfL), and 1L epitaxial graphene on BfL. (a) TEM micrograph of few layer epitaxial graphene on SiC. (b) Schematic of the structure of 1L + BfL epitaxial graphene film on SiC. (c) Raman spectrum of the bare SiC substrate and 1L epitaxial graphene film grown on SiC. The BfL-to-2L label indicates that while this film is mostly composed of 1L + BfL domains, regions of exposed BfL and 2L+BfL are also present.

defects in the lattice. The full width at half maximum of these two peaks is computed as approximately 15 cm^{-1} for the G peak and 50 cm^{-1} for the 2D peak, while the 2D/G integral intensity ratio is approximately 2. These results demonstrate that the film is composed of 1L graphene on BfL with regions presenting thicker graphene layers (2L + BfL) as well as uncovered BfL islands.

2.2 Å-indentation for transverse elasticity of 2D layers

Å-indentation is an Atomic Force Microscopy (AFM)-based force spectroscopy technique that allows sub-Ångström resolution indentation measurements [14]. This technique is particularly effective in measuring the transverse elasticity of 2D materials [20], due to indentation depths that are comparable to or smaller than the distance between 2D layers (sub-nano, e.g. interlayer distance in graphene is ~0.34 nm). Å-indentation experiments have enabled direct measurement of the interlayer properties of epitaxial graphene and graphene oxide [20], as well as the discovery of the ultra-stiff diamene film on few-layers epitaxial graphene [11] that we discuss in this report.

Å-indentation uses sub-Ångström vertical oscillations to measure the mechanical properties of 2D materials in the interlayer direction [20]. To this aim, a small sinusoidal voltage (<0.4 mV) is applied using a lock-in amplifier (Stanford Research Systems, SR830) to the piezotube of the AFM (Agilent PicoPlus AFM) to drive small oscillations Δz_{piezo} in parallel to the main AFM driving voltage, while the feedback loop of the AFM imposes a constant contact force F_z between tip and sample. The lock-in amplifier is used to drive the oscillation Δz_{piezo} of the cantilever-tip system and to control the variation in the normal force $\Delta F(F_z)$ associated to Δz_{piezo}. The stiffness of the contact $k_{cont} = (\Delta z_{piezo}/\Delta F(F_z) - 1/k_{lev})^{-1}$ is measured at different decreasing loads F_z (where k_{lev} is the spring constant of the AFM cantilever), to reconstruct the complete indentation curve. The indentation depth is obtained from Å-indentation data by computing the integral:

$$z_{\mathrm{indent}} = z_{P_0} + \int_{F_{P_0}}^{F'_z} \left(\frac{\Delta z_{\mathrm{piezo}}}{\Delta F(F'_z)} - \frac{1}{k_{\mathrm{lev}}} \right) dF'_z \qquad (1)$$

where F_{P0} is the pull-out force measured by the AFM when the tip loses contact with the sample's surface at z_{P0}. The classical Hertz model is used to estimate the stiffness of the contact, so that,

$$F_z = \frac{4E^*\sqrt{R}}{3} z_{\mathrm{indent}}^{3/2} \qquad (2)$$

where R is the tip radius and $E^* = ((1-\nu^2_{tip})/E_{tip} + (1-\nu^2)/E)^{-1}$ is the effective Young's modulus of the tip/sample contact, which depends on the elastic properties of the tip, namely the Young's modulus E_{tip} and Poisson's ratio ν_{tip}, and of the sample (ν, E). For more details on this experimental procedure and on the effect of adhesion forces we refer to the literature [14].

2.3 Automated nanomechanical characterization of graphene using machine learning

The topographic, friction force, and phase imaging data are collected on the same AFM by operating the instrument alternatively in contact and tapping mode. Nanosensors DT-NCHR polycrystalline diamond coated silicon tips are employed in all the experiments reported herein,

with resonant frequencies in the range 400-500 kHz, spring constant in the range 70-80 N/m, tip radius in the range 100-200 nm. Friction force microscopy (FFM) experiments are conducted in contact mode by scanning the sample with normal load in the range 20-300 nN and scan rates in the range 0.5 and 1.5 Hz. Notably, while a stiff tip (high spring constant) is not generally recommended for friction force microscopy, stiff tips are required for nanoindentation experiments and therefore are employed in our experiments. The frictional force is computed from AFM experiments by computing the difference between the lateral forces measured during the trace and retrace scan and by applying the formulas reported in references [21, 22]. Phase imaging experiments are conducted in tapping mode with the amplitude setpoint of the driving oscillation set in the range 0.4-0.6 A_0, with A_0 in the range 6-8 V. Following [23], the oscillation amplitude and phase can be related to the energy dissipated in the oscillation cycle, so that

$$E_h \propto A_0^2 \left(a\cos(\phi) - a^2\right) C_{\text{lev}} \qquad (3)$$

where E_h is the energy dissipated during oscillation, a is the amplitude setpoint (in the range 0.4-0.6 in our experiments), ϕ is the phase shift measured by the AFM, and C_{lev} is a constant that depends on the geometry and stiffness of the cantilever.

In order to detect the different graphene structures and estimate their nanomechanical properties, we employ a spectral clustering algorithm to analyze friction and phase imaging data. Spectral clustering is part of the broad category of unsupervised learning methods that are emerging in materials research [24, 25]. The goal of cluster analysis is to define subgroups or clusters in the data by employing pairwise similarities among the elements of the dataset. Clustering techniques, such as K-means and non-negative matrix factorization algorithm (NMF), have been recently employed in graphene research for the analysis of Raman spectra [26]. These data

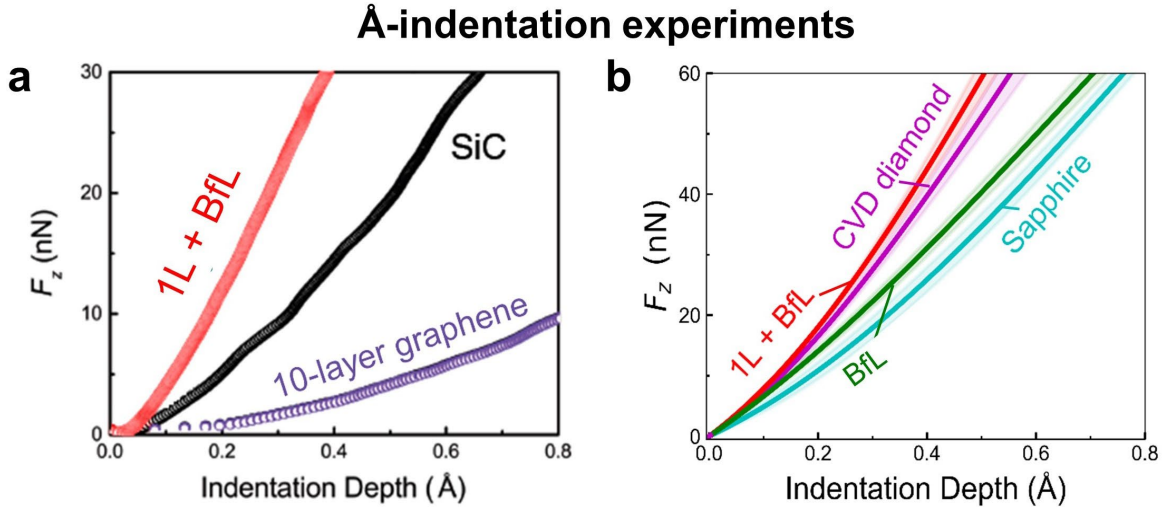

Figure 2. Å-indentation experiments conducted on 1L + BfL epitaxial graphene and other reference materials. (a) Å-indentation of 1L+BfL epitaxial films compared with indentation curves measured on bare SiC and 10-layer epitaxial graphene film grown on the C-face of SiC. (b) Å-indentation of 1L+BfL compared with indentation on bare BfL and reference stiff materials, namely HFCVD diamond microcrystals and bulk (0001) sapphire.

analysis methods can allow for automated determination of material properties in the presence of complex spatial distributions [27, 28], opening avenues for automated collection and analysis of AFM data. In this work, we employ a spectral clustering algorithm based on the Sklearn package in Python, and we refer to the literature for further details on this method [13, 29].

3. RESULTS

3.1 Å-indentation experiments

Å-indentation experiments are conducted to investigate the mechanical properties of few-layer graphene films epitaxially grown on the Si-face of SiC. In the same set of experiments, indentations are performed in the same conditions on materials with different mechanical properties in order to get a direct comparison and provide an internal reference for our measurements [14]. In Figure 2(a), we display the indentation curves measured on 1L + BfL graphene film grown on the Si-face of SiC and 10-layer epitaxial graphene film grown of the C-face of SiC , together with the indentation curve of pure SiC(0001). According to the Hertz equation (2), the slope of the indentation curves is proportional to the effective stiffness of the contact E^*, which in turn depends on the indentation modulus E of the material. The substantially steeper curve obtained for 1L + BfL graphene indicates that, at the nanoscale, the stiffness of this film appears to be much larger than the stiffness of the underlying 4H-SiC crystal. On the other hand, the film grown on the C-face of SiC (~10 layers thickness) presents a much softer interface, whose stiffness is comparable to the transverse stiffness of a graphite crystal (~33 GPa).

A possible explanation for the ultra-stiffness observed during nanoindentation of 1L + BfL films is the pressure-induced (~1-10 GPa) phase transition from graphene to a diamond-like structure, which is named diamene, whose crystalline structure is still under investigation [11]. Recent theoretical analysis have predicted that the formation of diamene is promoted by the stacking of graphene layers as well as by the saturation of the dangling bonds at the interface between SiC and BfL. Therefore, formation of diamene is deemed possible only in few layer graphene films (maximum two layer on top of BfL; however, experimental evidences have demonstrated that so far ultra-stiffness is not observed in 2L graphene + BfL) and is unlikely in graphene layers thicker than 5 and in epitaxial graphene films formed on C-face of SiC, which are known to present substantially different interlayer stacking than epitaxial graphene grown on Si-face. Recent reports have also found that the stiffening effect is not found in exfoliated graphene films on Silicon Oxide (SiO_2) [13], while pressure induced tuning of the electronic properties of exfoliated graphene films on SiO_2 has been demonstrated in Reference [30]. In the case of exfoliated films on SiO_2, the presence of –H and –OH groups naturally available at the interface of the 2D film at moderate humidity levels (>RH 35%) may enable the saturation of dangling bonds that are necessary for phase transformation [31]. However, these structures are unlikely to present ultra-high stiffness nor hardness, as observed in hydrogenated diamond-like carbon films [32].

In figure Figure 2(b), we display MoNI indentation curves measured on 1L + BfL epitaxial graphene and on bare BfL, together with reference indentation data measured for sapphire and HFCVD diamond microcrystals. Surprisingly, the slope of the indentation curve for 1L + BfL is comparable to the slope of the curve measure on the CVD diamond reference, showing that

diamene films may potentially have higher stiffness than bulk diamond at the nanoscale. This result is in line with micro-hardness experiments conducted on 1L + BfL films on SiC using a diamond indenter [20]. In these experiments, permanent indentation marks were produced on bare SiC by applying pressures on the order of 20 GPa using a sapphire AFM micro-cantilever equipped with a diamond Berkovich indenter. When the experiment was repeated in the same conditions on the 1L + BfL film on SiC, no residual deformation was found of the surface of the film. Experimental indentation curves in Figure 2(b) are used to evaluate the indentation modulus of the 1L + BfL film on SiC by direct comparison with the CVD diamond and sapphire references. The fitting of the data with Equation (2) is performed using a non-linear fitting in Python (for the polycrystalline diamond tip we assume E_{tip} =1050 and ν_{tip} = 0.115). From this analysis, we obtain a modulus of 1079 ± 69 GPa for the 1L + BfL film on SiC, which is comparable if not higher than the indentation modulus obtained for diamond crystals, and a modulus of 498 ± 26 GPa for the bare BfL on SiC.

3.2 Morphological analysis of epitaxial graphene surfaces using machine learning

The spectral clustering algorithm is used to identify the graphene domains in both friction force microscopy and phase imaging and to correlate these data with the topography of the film. In Figure 3(a), we display the topography of a 1L + BfL epitaxial graphene film grown on the Si-face of SiC. The topography presents terraces that are characteristic of the high-temperature annealing of SiC (the CCS process is conducted at temperatures on the order of 1500 ˚C, see Reference [6] for details on this process), with variable widths on the order of 1-2 μm. The

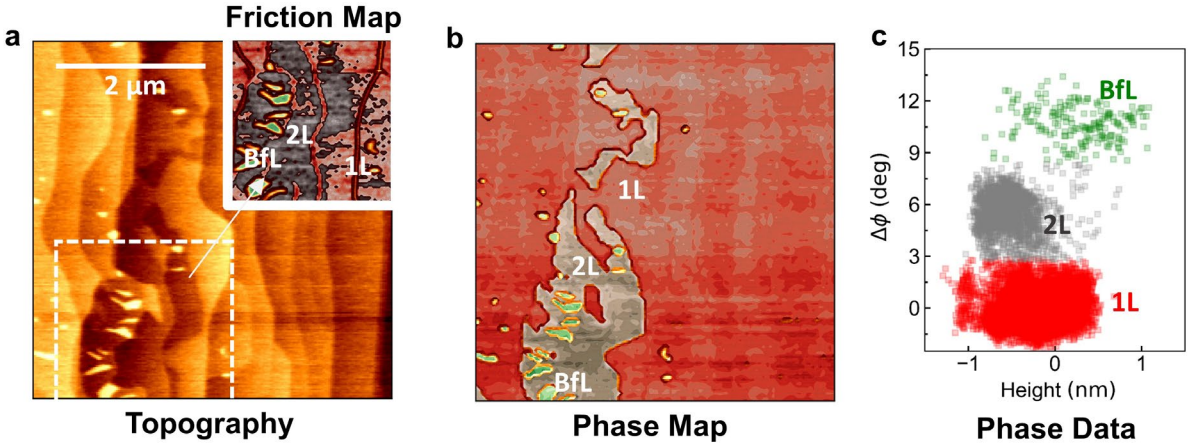

Figure 3. Topography and spectral clustering of friction and phase maps in 1L + BfL epitaxial graphene films on SiC. (a) Topography of a 1L+BfL epitaxial graphene region containing 2L + BfL and bare BfL islands. In the inset, spectral clustering of the friction force microscopy scan of the area identified by the dashed line on the topography. The different colors indicate domains assigned to BfL (green), 1L + BfL (red) and 2L + BfL (grey) by the spectral clustering algorithm. (b) Spectral clustering of the phase map obtained for the topographic image in (a). Colors indicate BfL (green), 1L + BfL (red) and 2L + BfL (grey) domain in the epitaxial film. (c) Scattering plot of the phase and height for BfL (green), 1L + BfL (red) and 2L + BfL (grey) extracted from the topography (a) and phase (b) maps using the clustering algorithm.

formation of the terraces, together with the complex morphology of the graphene films grown on their surface, makes the detection of the different graphene domains (namely, BfL, 1L and 2L) quite a challenging task from the sole topography data.

In the inset of Figure 3(a), we display the results obtained for clustering frictional data in the regions identified by the squared box in the bottom left side of the topography image through the spectral clustering algorithm, which allows for fast and robust identification of the 1L + BfL, 2L + BfL, and bare BfL domains. More importantly, the clustering algorithm directly evaluates frictional forces in the different domains, estimating their distributions, means, and standard deviations. For this experiment, we obtain a resulting friction force of 16±2 nN on BfL, 1.7±0.5 nN for 1L + BfL, and 1.2±0.3 nN for 2L + BfL. We find that friction forces on BfL are more than ten-fold higher than friction of 1L + BfL; the higher friction forces on BfL compared to graphene domains can be attributed to the roughness of this layer as well as the effect of the covalent bonding to the SiC substrate [18]. A decrease of the frictional force is observed between 1L + BfL and 2L + BfL graphene, which is related to a decrease of vibrational dissipation with the increasing number of layers [33], even though the contribution of capillary and adhesion forces to the overall friction force cannot be excluded, give that experiments are conducted in air at humidity level of ~40% RH.

In Figure 3(b), we display the results obtained for clustering phase imaging data using a combined dataset composed of topography data in Figure 3(a) and phase imaging data. The spectral clustering algorithm is able to isolate with great accuracy the different graphene domains in perfect accordance with the clustering results obtained for friction force data in the inset of Figure 3(a). Figure 3(c) reports the distributions of topographical height and phase shift obtained from the spectral clustering algorithm in the scan region (due to the presence of a variable offset in the phase measurement, phase values are reported as the relative differences from the phase of 1L + BfL film, which is set to 0 deg). Notably, a substantial phase shift is observed in BfL domains, which may be associated with larger energy dissipation on this rough region (see equation 3). The difference in phase shift between 1L + BfL and 2L + BfL films may also be associated to a difference in the energy dissipated with varying number of layers, further analysis of this result is still ongoing. This methodology shows great promise for the development of automated analyses of surface properties using AFM, as well as providing a tool for definition of nanomechanical data clusters at the nanoscale.

4. CONCLUSIONS

The surprising mechanical properties of few-layer graphene-diamene films, exhibiting hardness and stiffness at the nanoscale comparable or even higher than those of bulk diamond, show great potential for new developments in the field of hard coatings, with applications reaching different technological fields beyond mechanical technology. Experiments on the mechanical properties of these materials are underway, with the goal of transferring this technology from the nanoscale to large scale applications. To this aim, the development of automated identification techniques and machine learning methods, which can independently extract information of these films and assess their composition, can represent an important step toward improving the research and development process and increase our chances to move faster from the lab bench to relevant industrial applications.

AKNOWLEDGMENTS

The Authors acknowledge the support from the Office of Basic Energy Sciences of the US Department of Energy (grant no. DE-SC0018924). Epitaxial graphene samples used in the experiments described herein have been prepared by Professor Walt de Heer at the Georgia Institute of Technology and Dr. Claire Berger at the Institut Néel, CNRS-University Grenoble-Alpes. This research would not have been possible without their contribution.

REFERENCES

1. Mas-Balleste, R., et al., *2D materials: to graphene and beyond.* Nanoscale, 2011. **3**(1): p. 20-30.
2. Akinwande, D., et al., *A review on mechanics and mechanical properties of 2D materials—Graphene and beyond.* Extreme Mechanics Letters,, 2017. **13**: p. 42-77.
3. Palaci, I., et al., *Radial elasticity of multiwalled carbon nanotubes.* Physical Review Letters, 2005. **94**(17).
4. Lucas, M., et al., *Aspect ratio dependence of the elastic properties of ZnO nanobelts.* Nano letters, 2007. **7**(5): p. 1314-1317.
5. Novoselov, K.S., et al., *Two-dimensional atomic crystals.* Proceedings of the National Academy of Sciences, 2005. **102**(30): p. 10451-10453.
6. de Heer, W.A., et al., *Large area and structured epitaxial graphene produced by confinement controlled sublimation of silicon carbide.* Proceedings of the National Academy of Sciences, 2011. **108**(41): p. 16900-16905.
7. Novoselov, K.S., et al., *2D materials and van der Waals heterostructures.* Science, 2016. **353**(6298): p. aac9439.
8. Martins, L.G.P., et al., *Raman evidence for pressure-induced formation of diamondene.* Nature Communications, 2017. **8**(1): p. 96.
9. Rajasekaran, S., et al., *Interlayer carbon bond formation induced by hydrogen adsorption in few-layer supported graphene.* Physical review letters, 2013. **111**(8): p. 085503.
10. Lu, S., et al., *High pressure transformation of graphene nanoplates: A Raman study.* Chemical Physics Letters, 2013. **585**: p. 101-106.
11. Gao, Y., et al., *Ultrahard carbon film from epitaxial two-layer graphene.* Nature Nanotechnology, 2018. **13**(2): p. 133-138.
12. Cellini, F., et al., *Epitaxial two-layer graphene under pressure: Diamene stiffer than Diamond.* FlatChem, 2018. **10**: p. 8-13.
13. Cellini, F., et al., *Layer dependence of graphene-diamene phase transition in epitaxial and exfoliated few-layer graphene using machine learning.* arXiv preprint arXiv:1901.09071, 2019.
14. Cellini, F., Y. Gao, and E. Riedo, *Å-Indentation for non-destructive elastic moduli measurements of supported ultra-hard ultra-thin films and nanostructures.* arXiv:1901.09059 2019.
15. Narayan, J., et al., *Q-carbon harder than diamond.* MRS Communications, 2018: p. 1-9.
16. Berger, C., et al., *Electronic confinement and coherence in patterned epitaxial graphene.* Science, 2006. **312**(5777): p. 1191-1196.
17. Yazdi, G.R., et al., *Growth of large area monolayer graphene on 3C-SiC and a comparison with other SiC polytypes.* Carbon, 2013(477-484).

18. Conrad, M., et al., *Structure and evolution of semiconducting buffer graphene grown on SiC(0001).* Physical Review B, 2017. **96**(19): p. 195304.
19. Röhrl, J., et al., *Raman spectra of epitaxial graphene on SiC (0001).* Applied Physics Letters, 2008. **92**(20): p. 201918.
20. Gao, Y., et al., *Elastic coupling between layers in two-dimensional materials.* Nature Materials, 2015. **14**(7): p. 714-720.
21. Xie, H., et al., *Calibration of lateral force measurements in atomic force microscopy with a piezoresistive force sensor.* Rev Sci Instrum, 2008. **79**(3): p. 033708.
22. Liu, W., K. Bonin, and M. Guthold, *Easy and direct method for calibrating atomic force microscopy lateral force measurements.* Rev Sci Instrum, 2007. **78**(6): p. 063707.
23. Stark, M., et al., *From images to interactions: high-resolution phase imaging in tapping-mode atomic force microscopy.* Biophys J, 2001. **80**(6): p. 3009-18.
24. Hastie, T., R. Tibshirani, and J. Friedman, *The Elements of Statistical Learning*. 2017: Springer.
25. Jain, A.K., *Data clustering: 50 years beyond K-means.* Pattern Recognition Letters, 2010. **31**(8): p. 651-666.
26. Kunc, J., et al., *A method to extract pure Raman spectrum of epitaxial graphene on SiC.* Applied Physics Letters, 2013. **103**: p. 201911.
27. Somnath, S., et al., *Feature extraction via similarity search: application to atom finding and denoising in electron and scanning probe microscopy imaging.* Advanced Structural and Chemical Imaging, 2018. **4**(1).
28. Yen, C.F. and S. Sivasankar, *Improving estimation of kinetic parameters in dynamic force spectroscopy using cluster analysis.* Journal of Chemical Physics, 2018. **148**(12).
29. Pedregosa, F., et al., *Scikit-learn: Machine Learning in Python.* Journal of Machine Learning Research, 2011. **12**(2825-2830).
30. Ares, P., et al., *Tunable Graphene Electronics with Local Ultrahigh Pressure.* Advanced Functional Materials, 2019: p. 1806715.
31. Barboza, A.P., et al., *Room-temperature compression-induced diamondization of few-layer graphene.* Advanced Materials, 2011. **23**(27): p. 3014-3017.
32. Robertson, J., *Diamond-like amorphous carbon.* Materials science and engineering: R: Reports, 2002. **37**(4): p. 129-281.
33. Filleter, T., et al., *Friction and dissipation in epitaxial graphene films.* Physical Review Letters, 2009. **102**(8).